ELSEVIER

Journal of South American Earth Sciences 25 (2008) 492–500

Journal of
South American
Earth Sciences

www.elsevier.com/locate/jsames

Genetic and metamorphic conditions constrained by fluid inclusions from Paleoproterozoic (c. 1.8 Ga) magnesite ore deposits, NE Brazil

Luiz Henrique Ronchi [a,*], Clóvis Vaz Parente [b], Kazuo Fuzikawa [c], Artur Bastos Neto [d]

[a] *Programa de Pós-Graduação em Geologia, Universidade do Vale do Rio dos Sinos–UNISINOS, Av. Unisinos, 950, 93 022 000 São Leopoldo, RS, Brazil*
[b] *Departamento de Geologia, Universidade Federal do Ceará–UFC, Campus Universitário do Pici, 60 455 760 Fortaleza, CE, Brazil*
[c] *Comissão Nacional de Energia Nuclear, Centro de Desenvolvimento da Tecnologia Nuclear, Supervisão de Física Aplicada e Técnicas Especiais Ct2–CNEN, Rua Mário Werneck, s/n (Campus UFMG) Pampulha, 31 270 010 Belo Horizonte, MG, Brazil*
[d] *Universidade Federal do Rio Grande do Sul–UFRGS, Instituto de Geociências, Av. Bento Gonçalves, 9500, 91 501 970 Porto Alegre, RS, Brazil*

Received 10 October 2005; accepted 20 August 2007

Abstract

Precambrian magnesite occurrences hosted by metadolomites from the Orós belt, Ceará, Brazil, are part of a greenschist–amphibolite, metavolcano-sedimentary terrain, dated at 1.8 Ga, cut by Meso- to Neoproterozoic Brasiliano granites and Neoproterozoic basic sills. These rocks were affected by a shear zone between 580 and 500 Ma. The magnesite-bearing marbles can be grouped as medium-grained (1–9 mm) at the Riacho Fundo ore deposit or sparry magnesite (1–15 cm) at the Cabeça de Negro ore deposit. The sparry magnesite shows textural characteristics related to original sedimentary structures. Both types of magnesite-bearing marbles contain aqueous and aqueous-carbonic fluid inclusions that yield homogenization temperatures between 170 and 370 °C. Applying a pressure correction, these temperatures are compatible with the evolution from greenschist to amphibolite facies metamorphic conditions, as described in previous work on the Orós region. It also agrees with data in specialized literature on the metamorphism of carbonate rocks. Fluid inclusion distribution, composition, and physical-chemical characteristics suggest temperature increase, probably related to metamorphism on these rocks. The medium-grained magnesite records partial contamination of CO_2-rich inclusions by relict carbonaceous material (bitumen, hydrocarbons?) that favors, but does not confirm, a syngenetic sedimentary origin and could have caused the lowering of CO_2 melting point in these inclusions. Therefore, though textural evidence points to a sedimentary-diagenetic model, fluid inclusions record conditions of a metamorphic event.

Keywords: Magnesite; Fluid inclusions; Metamorphism; Orós belt

Resumo

As ocorrências de magnesita pré-cambriana encaixadas em metadolomitos do cinturão Orós, Ceará, Brasil, fazem parte de um terreno metavulcano-sedimentar de fácies xisto verde a anfibolito, com idade de 1,8 Ga, cortado por granitos meso a neoproterozóicos relacionados ao Ciclo Brasiliano e *sills* básicos neoproterozóicos. O conjunto foi afetado por zonas de cisalhamento por volta de 580–500 Ma. Os corpos de magnesita podem ser separados em dois grupos: magnesita de grão médio (1 a 9 mm) no depósito de Riacho Fundo e espática (1 a 15 cm) no depósito de Cabeça de Negro. A espática apresenta grande variação textural claramente relacionada a estruturas originalmente sedimentares. Ambos os tipos de mármores magnesíticos possuem inclusões fluidas aquosas primárias e secundárias, além de aquo-carbônicas, que apresentam temperaturas de homogeneização entre 170 e 370 °C. Com a correção de pressão essas temperaturas são compatíveis com condições metamórficas evoluindo da fácies xisto verde para anfibolito tal como descrito na região de Orós e na

* Corresponding author. Tel.: +55 51 35 91 11 22; fax: +55 51 35 90 81 77.
E-mail address: ronchi@unisinos.br (L.H. Ronchi).

0895-9811/$ - see front matter © 2007 Elsevier Ltd. All rights reserved.
doi:10.1016/j.jsames.2007.10.005

literatura especializada sobre metamorfismo de rochas carbonáticas. As características físico-químicas, composição e distribuição sugerem aumento de temperatura aparentemente ligado ao metamorfismo amplamente reconhecido dessas rochas. Na magnesita de grão médio nota-se a contaminação parcial de inclusões ricas em CO_2 por material carbônico reliquiar (betume, hidrocarboneto?) o que favorece, embora não confirme, a hipótese singenética sedimentar e é também responsável pelo rebaixamento da temperatura de fusão do CO_2 das inclusões aquo-carbônicas. Portanto, embora existam evidências texturais relacionadas a um modelo genético sedimentar-diagenético, as inclusões fluidas registram as condições do evento metamórfico.

Palabras Claves: Magnesite; Fluid inclusions; Metamorphism; Orós belt

1. Introduction

Deposits of sparry and microcrystalline magnesite are usually found associated with deformed and metamorphosed carbonate rocks, in which primary depositional textures and structures are partially or no longer preserved. A controversy therefore arose, related to two genetic models proposed for magnesite deposits. In the syngenetic model, primary sedimentary deposits can be formed by *in situ* chemical precipitation, which involves deposition of microcrystalline or sparry magnesite, followed by epigenesis (Morteani, 1989). The second model involves deposition from hydrothermal fluids, in which metasomatic replacement with introduction of Mg^{2+} in a precursor carbonate creates sparry textures through recrystallization (Dabitzias, 1980; Bone, 1983; Lugli et al., 2002; Fernandez-Nieto et al., 2003). Fluid inclusion studies may address these issues through the characterization of physical–chemical conditions of the solution associated with the minerals, but superimposed metamorphic processes on these magnesite lenses may have destroyed evidence in the primary fluid.

The main stratiform magnesite ore deposits in the Orós belt, northeastern Brazil (Torto, Alencar, and Cabeça de Negro), are active, productive mines, whereas Riacho Fundo and Malhada Vermelha are nonproductive ore deposits (Fig. 1). Registered ore reserves are of 264,639,144 tons.

The magnesite bodies are part of a greenschist to amphibolite facies, metavolcano-sedimentary terrain. The enclosing metasedimentary rocks comprise a metacarbonate sequence with lenses of magnesite-bearing marbles that extend more than 140 km (Parente et al., 1998a, 1998b). Magnesite-bearing marbles are composed of medium-grained (1–9 mm) or sparry (1–15 cm) magnesite. According to Parente et al. (2004), the magnesite marbles are of sedimentary origin, having undergone important diagenetic evolution before the metamorphic event that took place during the Neoproterozoic Brasiliano orogenic cycle.

The present fluid inclusion study was carried out in metamorphic samples from two magnesite deposits, Riacho Fundo (medium-grained magnesite) and Cabeça de Negro (sparry magnesite). The aim was to define which solutions are associated with the different magnesite ore deposits, as well as to understand how they could relate to the magnesite genetic controversy.

2. Geological setting

The magnesite ore deposits are hosted by the Orós Complex, which is part of a Proterozoic foldbelt from the Borborema Province, NE Brazil. It is a metavolcano-sedimentary sequence, intruded by Meso- to Neoproterozoic granites during the Brasiliano orogeny and basic to ultrabasic Neoproterozoic rocks. Metarhyolites intercalated with the metasedimentary rocks yield an age of approximately 1.8 Ga (Sá, 1991; Van Schmus et al., 1995). The metasedimentary rocks comprise mainly mudstones, represented by aluminous schists, frequently intercalated with quartzites. They are partially covered by evaporites and marine carbonates composed of calcite, dolomite, magnesite-rich marbles, and calc-silicate rocks. Feldspathic schists and metagraywackes superpose the latter (Fig. 1). Carbon and oxygen isotope data from calcite and dolomite marbles reported by Parente et al. (2004), despite some modification during metamorphism, suggest that the deposition took place in a confined or shallow marine environment. The volcano-sedimentary sequence was deformed into narrow isoclinal folds, with vertical axial plane foliation and subhorizontal stretching lineations, compatible with the Brasiliano orogeny transpressive regime (Sá, 1991; Parente and Arthaud, 1995). This sequence was metamorphosed under greenschist to amphibolite facies conditions. Thermobarometric data in magnesite-bearing schists suggest a temperature range between 443 and 507 °C for aluminous schists with staurolite and between 436 and 485 °C for aluminous schists without staurolite, with pressures of nearly 3 kbar (Sá, 1991). Parente (1995) estimates metamorphic conditions between 450 and 480 °C and 2–5 kbar using tremolite–talc–dolomite–calcite–quartz and tremolite–diopside–dolomite–quartz–calcite assemblages in the sparry and medium-grained magnesite marbles, respectively.

The dextral Orós shear zone is superimposed almost synchronically onto the main metamorphic foliations of the metavolcano-sedimentary rocks. This heterogeneous ductile deformation is characterized by subvertical mylonitic foliation, subhorizontal lineation, transposition of the foliation parallel to the mylonitic fabric, C/S fabric surfaces, and C'-type shear band cleavage planes that are more conspicuous in the ortho-derived rocks than in the metasedimentary rocks. In carbonatic rocks, particularly magnesite marbles, the following shear features are distinguished: (1) sigmoidal structures in micro and mega-scales; (2) boudi-

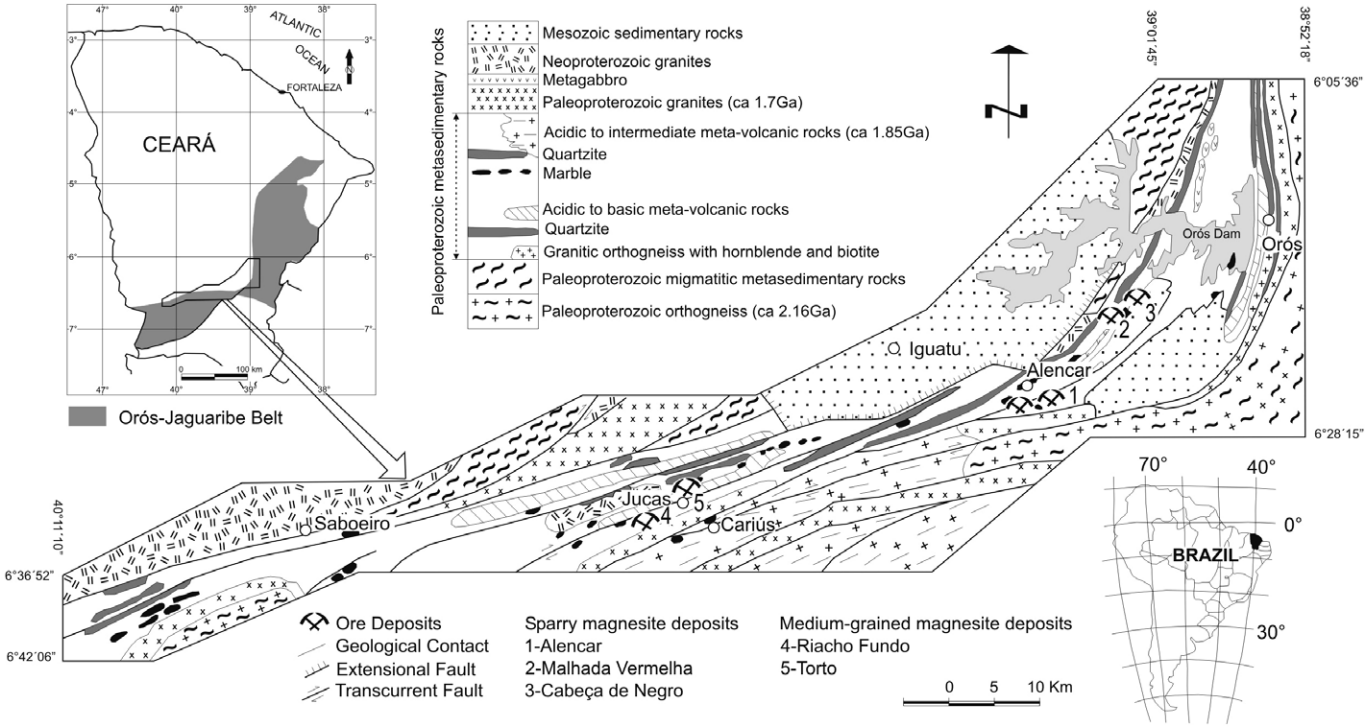

Fig. 1. Location and regional geologic map of magnesite-bearing rocks in the Orós belt. Modified after Sá (1991) and Parente (1995).

nage structures from micrometric to metric scales, where the magnesite bodies hosted either by metadolomite (e.g., Cabeça de Negro Ore deposit) or by chlorite and talc-rich beds (e.g., Riacho Fundo Ore deposit) are the less deformed rocks, because magnesite is more resistant to deformation than metadolomite, and the latter are more resistant than the magnesian phyllosilicates; and (3) protomylonitic texture marked by subangular to subrounded magnesite porphyroclasts in a granoblastic mosaic of smaller magnesite grains, related to dynamic recrystallization, as observed in the studied samples (see number 5 in Fig. 4). The porphyroclasts are usually stretched, with sutured contacts, deformation bands, undulatory extinction, and extensional fissures.

Dating of the Borborema province shear zone indicates Brasiliano ages and that the zone was active from 580 to 500 Ma according to $^{40}Ar/^{39}Ar$ data (Feraud et al., 1992).

2.1. Description of sparry magnesite ore deposits

Sparry magnesite ore deposits (Alencar, Malhada Vermelha, and Cabeça de Negro) are hosted by dolomite marbles that locally contain lutecite, scapolite, and pseudomorphic sulfate nodules after quartz, dissolution breccias, and petal-shaped texture. This association indicates deposition under evaporitic conditions. Transition from sparry magnesite to dolomite marbles is usually gradual and well defined, though it may become complex if a mixture between these carbonate rocks is observed. This observation may suggest either contemporaneous deposition or an incomplete replacement process. Sparry magnesite veins may cut metadolomites as well.

Magnesite marbles show large textural variations, including porphyroblastic, rosette, banded, and palisadic textures. In spite of the metamorphic changes undergone by these rocks, the banded and palisadic types are preserved sedimentary structures. Stromatolites and subrounded concentric microfossils devoid of carapace and with sizes from 200 to 300 μm are associated with banded textures. Similar microfossils were described by Chaye d'Albissin and Guillou (1985) as accumulated in an originally colloidal magnesite deposit and preserved as fossils in magnesite crystals through diagenetic and metamorphic processes.

Rock color ranges from white to light grey, dark grey, and red. Sparry magnesite crystals (1–15 cm) are usually subautomorphic and frequently deformed, showing formation of subgrain and comminution. Magnesite is the main mineral phase associated with chlorite, talc, pyrite, and iron oxides. Some magnesite layers are silica rich (up to 21%), with talc and chlorite, whereas others are rich in iron oxides.

Magnesite in the Cabeça de Negro deposit is hosted by metadolomites that display boudinage in both mega- and microstructures. The magnesite-bearing marbles are the most competent (less deformed) rocks. These lenses are characterized by palisadic and rhythmic structures that represent carbonate sedimentation. Such variations could be linked to sea-level changes. Magnesite and metadolomites enriched in iron oxide, aluminium silicate, and sometimes detrital zircon are also found in the deposit; these features may represent freshwater inflow (Parente et al., 2004).

2.2. Description of medium-grained magnesite ore deposits

Medium-grained magnesite marbles occur in two bodies, Riacho Fundo and Torto. This rock is relatively more homogeneous in texture and color than the sparry magnesite ore deposit. Magnesite crystals are usually xenomorphic.

The Riacho Fundo deposit is an irregular lens that comprises a pinch-and-swell megastructure partially deformed by a ductile shear zone. Light-grey metadolomites, biotite-phlogopite-tremolite schists, and scapolite-bearing calc-silicate rocks enclose it.

Magnesite marbles display a predominant fine to medium granular texture (1–8 mm) and white color, with grey stains marking the presence of silicate minerals. Slight textural/structural variations occur locally, such as concentric structures, 3–6 mm in diameter, immersed in a talc–chlorite matrix, or extensional and shear veins filled with 1 cm prismatic and translucent magnesite crystals, forming symmetric comb structures. The latter also occurs in a talc–chlorite host.

Fine to medium granular marbles display granoblastic to allotriomorphic textures essentially composed of magnesite. Accessory minerals include talc, chlorite, and pyrite. The magnesite crystals are usually deformed, 0.02–8 mm in size. The largest crystals have sutured borders, undulatory extinction, deformational bands, and subgrain recrystallization. These features are clouded by roughly oriented or randomly distributed dark inclusions (organic matter-like?). Conversely, the small crystals are usually pure, with straight or slightly curved borders and triple junctions. Therefore, the largest crystals likely are synmetamorphic, whereas the small, more abundant ones are possibly the product of dynamic recrystallization.

3. Fluid inclusions

3.1. Samples and techniques

For fluid inclusion studies, 22 doubly polished sections of metadolomites, sparry, and medium-grained magnesites were prepared, including different textural and structural types. However, only one magnesite sample from the Riacho Fundo (medium-grained) and one from the Cabeça de Negro (sparry) deposits contain fluid inclusions with appropriate size, transparency, and quantity for detailed studies. No suitable inclusions were found in metadolomite samples. Petrographic studies were used for determination and classification of the several fluid inclusion types, subsequently characterized by microthermometric runs and Raman spectroscopy. The latter technique used a Dilor Raman multichannel spectrometer from the Physics Institute of the Universidade Federal de Minas Gerais. A Chaix Meca freezing–heating stage, calibrated at CO_2 and H_2O triple points and by the final melting temperatures of Merck standards (135, 200, 306, and 398 °C), was used to collect microthermometric data. Estimated precision for the measurements is nearly 0.2 °C, and accuracy is ± 0.5 °C at temperatures up to 135 °C, steadily increasing to up to 12 °C at temperatures of 398 °C. To compare and confirm the obtained microthermometric data, independent runs were carried out in another Chaix Meca stage at the Universidade Federal do Rio Grande do Sul (Porto Alegre), as well as in an USGS stage at CNEN (Comissão Nacional de Energia Nuclear), Belo Horizonte, with consistent results. Bodnar (2003) equations of state were used for salinities calculations, determined from ice-melting temperatures, and from clathrate dissolution. Brown and Lamb (1986) data were used with the aid of MacFlincor software (Brown and Hagemann, 1994).

3.2. Medium-grained magnesite from the Riacho Fundo deposit

In the Riacho Fundo deposit, medium-grained metamorphic magnesite presents successive growth zones with solid and fluid inclusions. Some inclusions display a regular distribution of the zones (Fig. 2). Zone 1 is clear, without solid or fluid inclusions. Zone 2 is thin, consisting of primary aqueous two-phase inclusions, with polygonal shapes, sizes up to 30 μm, and walls parallel to the growth zones. Eventual one-phase aqueous inclusions may occur, associated with aqueous two-phase inclusions. These inclusions probably result from metastable conditions or necking down. Zone 3 is a large central band, showing round to oval dolomite solid inclusions, as determined by Raman spectrometry. These inclusions are locally associated with three-phase aqueous-carbonic fluid inclusions. The size and shape of the cavities may vary to up to 30 μm. The distribution of these inclusions is roughly parallel to the magnesite growth bands, suggesting a primary genetic classification. Finally, the thin band with aqueous two-phase inclusions (Zone 2) and the clear zone without solid or fluid inclusions (Zone 1) repeat. In nearby crystals, there are rough trails of round, secondary, aqueous, two-phase fluid inclusions that cut across magnesite and show signs of necking down. The aqueous two-phase fluid inclusions also can be found in other sharper trails that cross-cut several crystals with the same characteristics, of secondary later origin.

Investigations of CO_2 and CH_4 were performed with Raman microspectroscopy. At least one aqueous liquid inclusion bears traces of CO_2 and N_2; only CO_2 was detected in aqueous-carbonic inclusions, and CH_4 or N_2 were not detected in these inclusions.

Another type of inclusion is partially or totally filled with a black opaque viscous material, sometimes associated with solid round dolomite inclusions. Its shape is usually round, with small clear aqueous appendices (Fig. 3). It probably corresponds to the organic matter clouds (carbon). The black phase is usually smaller than 5 μm, and its composition could not be determined by Raman microspectrometry because of the high fluorescence of this phase, which completely hinders the Raman signal (Pironon,

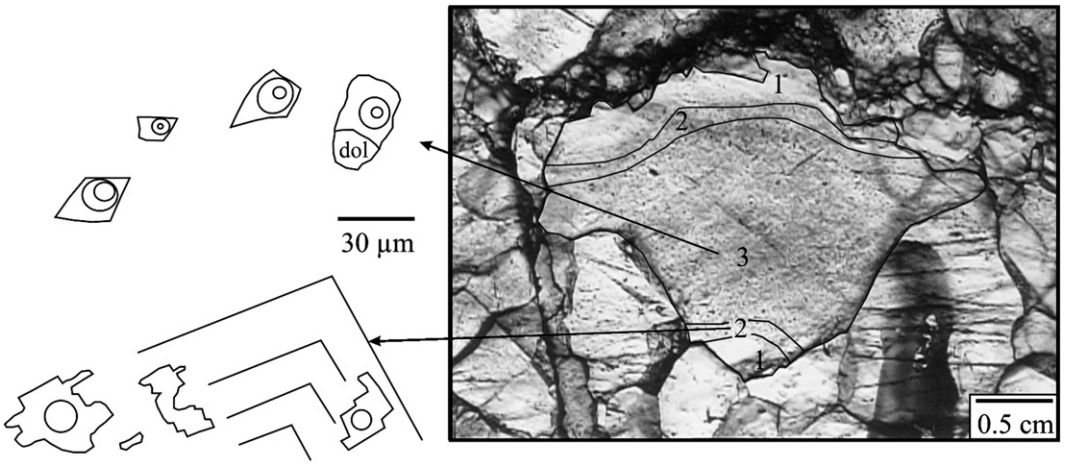

Fig. 2. Magnesite crystal (right) showing a succession of three metamorphic growth zones with different fluid inclusion types represented on left side. Zone 1: clear band devoid of fluid inclusions; Zone 2: one- and two-phase aqueous fluid inclusions; orthogonal lines represent growth bands; Zone 3: aqueous-carbonic fluid inclusions with and without dolomite (dol) as accidental solid inclusion (modified from Parente et al., 2004).

1991). This phenomenon is characteristic of hydrocarbon-rich inclusions (Kerkhof, 1988), not of carbon-rich ones, which display peaks at 1300 and 1580 cm^{-1} (Ronchi and Bény, 1997), or of graphite, which has two sharp peaks at 1582 and 140 cm^{-1} (McMillan, 1989). Had the inclusions been greater than 15 μm, their composition could have been determined by infrared microspectrometry, but such was not the case (Pironon et al., 1991). Evidence of their viscous consistency was determined during Raman spectrometry, when the passage of laser rays created a hole that spontaneously closed after a few weeks. This development may suggest the presence of bitumen in the inclusions.

All primary or secondary fluid inclusions are located in metamorphic magnesite crystals. In addition, very small (<5 μm), aqueous, one-phase and two-phase inclusions compose sharply contrasting secondary trails.

3.3. Sparry magnesite from the Cabeça de Negro deposit

Fluid inclusions in sparry magnesite are similar to those described in the Riacho Fundo deposit but with different proportions. Aqueous inclusions are predominant in the Riacho Fundo deposit, whereas in the Cabeça de Negro deposit, aqueous-carbonic, three-phase inclusions are the most common. Fig. 4 displays the typical mode of occurrence of these inclusions: a longitudinal trail with aqueous-carbonic, three-phase inclusions (1) that terminates within a single crystal. These are probably pseudo-second-

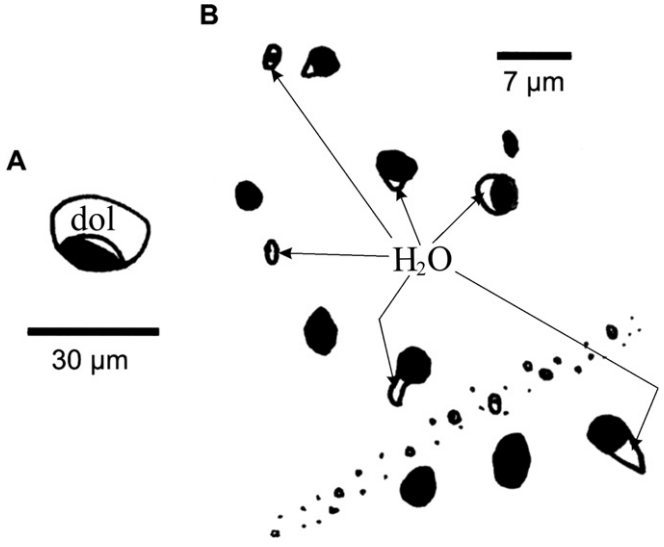

Fig. 3. (A) Round solid dolomite (dol) inclusion associated with a black phase, probably organic matter, and a thin, clear aqueous component. (B) Black opaque inclusions with clear aqueous appendices. Note the presence of a small secondary aqueous fluid inclusion trail and one-phase and two-phase aqueous inclusions associated with the black inclusions (modified from Parente et al., 2004).

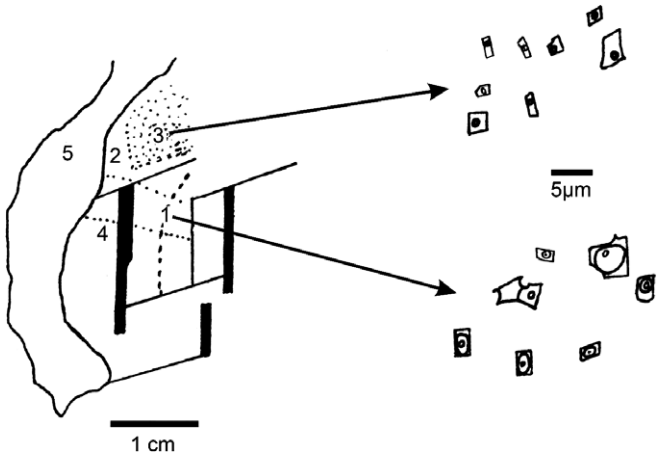

Fig. 4. Fluid-inclusion types from the Cabeça de Negro sparry deposit: (1) pseudo-secondary aqueous-carbonic inclusions; (2) magnesite inclusion-free growth band; (3) primary aqueous two-phase fluid inclusions; (4) translucent, fine, and white, inclusion-free magnesite; (5) fine, white and translucent, fluid-inclusion free magnesite (modified from Parente et al., 2004).

ary inclusions (Roedder, 1984). In the crystal immediately above, two zones occur: a clear, fluid-inclusion free growth zone (2) and other zones with aqueous, two-phase fluid inclusions showing negative crystal shapes with random distribution; these are probably primary inclusions (3). Along the trail in Fig. 4, tiny (<2 μm) cavities occur (4) transverse to the tabular magnesite crystal. These are aqueous, one- or two-phase secondary inclusions. A fine, white, translucent, fluid-inclusion free magnesite also occurs (5), a product of dynamic recrystallization, probably linked to the shear zone. Usually there are a few dolomite solid inclusions and no hydrocarbons.

3.4. Microthermometry on the Riacho Fundo deposit

CO_2 melting temperatures in medium-grained magnesite samples were mainly around −56.6 °C, though some inclusions display CO_2 melting temperatures lower than −56.6 °C, mostly −59.0 °C. These temperatures suggest the presence of other volatiles, such as CH_4, unfortunately not detected by Raman analysis (Fig. 5). It was not possible to observe the temperature of clathrate dissolution and thus obtain true salinity values for the aqueous phase of these inclusions. Homogenization temperatures of the CO_2 phase into liquid state ranged 27–28 °C. During heating, a major proportion of the fluid inclusions decrepitated. Three fluid inclusions displayed total homogenization temperature in the range of 350–360 °C, one at 210 °C, and another at 160 °C.

Traces of CO_2 were detected by Raman spectrometry in some aqueous inclusions, but these inclusions do not show a visible phase change at −56.6 °C or clathrate formation. Final ice melting temperatures from −3.0 to −5.8 and −12.6 to −15.4 were distributed between two groups (Table 1) with different salinities: one with nearly 7 wt% NaCl equiv. (primary aqueous inclusions), and another with 17.5 wt% NaCl equiv. (secondary aqueous inclusions). Homogenization temperatures (Fig. 6) ranged from 290 to 360 °C, with a concentration around 340–360 °C (14 runs out of 32). The arithmetic mean is 353 °C for the high-salinity secondary inclusions and

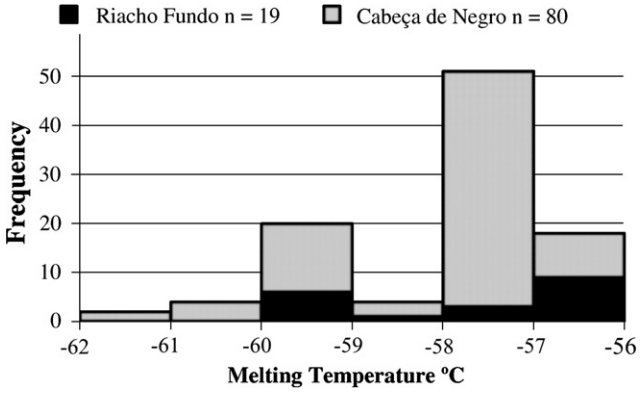

Fig. 5. Histogram of CO_2 melting temperatures.

Table 1
Microthermometric and calculated salinity data

Ore deposit	FI type	$TmCO_2$			TmH_2O			Sal			Td_{clat}			$ThCO_2$			Th_{tot}		
		Min	Max	Med	Min	Max	Med	Min	Max	Med	Min	Max	Med	Min	Max	Med	Min	Max	Med
Riacho Fundo																			
	Aqueous primary	–	–	–	−3.0	−5.8	−4.4	5.0	9.0	7.0	–	–	–	–	–	–	171.5	395.0	283.0
	Aqueous secondary	–	–	–	−12.6	−15.4	−13.7	16.5	19.0	17.5	–	–	–	–	–	–	146.0	358.5	353.0
	Aqueous carbonic	−61.6	−56.6	−58.5	–	–	–				–	–	–	24.7	31.1	29.0	127.2	372.5	307.9
Cabeça de Negro																			
	Aqueous primary	–	–	–	−3.0	−6.6	−5.1	5.0	10.0	8.0	–	–	–	–	–	–	232.5	271.0	250.5
	Aqueous secondary	–	–	–	−12.6	−14.8	−14.3	16.5	18.5	18.0	–	–	–	–	–	–	236.0	262.0	249.0
	Aqueous carbonic	−60.7	−56.6	−57.5	–	–	–	2.3	13.0	6.0	2.0	8.8	6.8	6.5	31.1	25.0	290.0	387.5	335.0

Min, minimum temperature registered; max, maximum temperature registered; med, medium temperature registered. $TmCO_2$, CO_2 melting temperature °C; TmH_2O, last ice melting temperature °C; Sa, salinity wt% NaCl equiv.; Td_{clat}, clathrate dissolution temperature °C; $ThCO_2$, CO_2 phase partial homogenization temperature °C; Th_{tot}, total homogenization temperature °C.
Aqueous carbonic inclusions are primary.

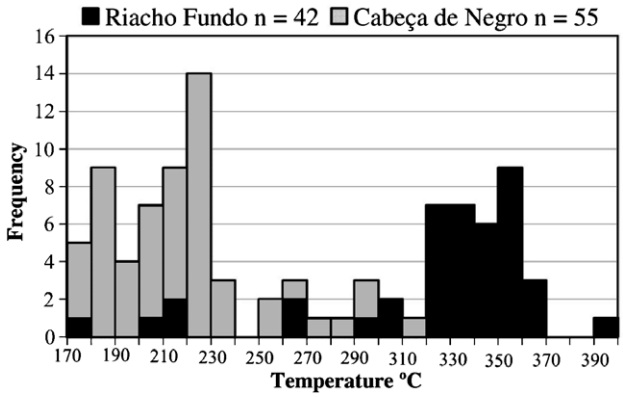

Fig. 6. Histogram of total homogenization into liquid state of the two-phase aqueous fluid inclusions.

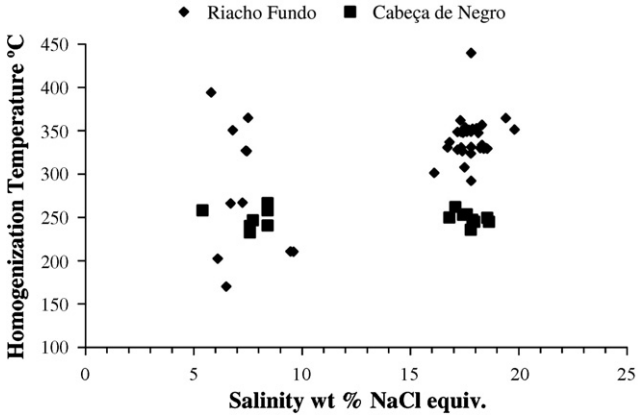

Fig. 7. Homogenization temperature–salinity plot for primary and secondary two-phase aqueous fluid inclusions from the Riacho Fundo and the Cabeça de Negro magnesite deposits. Low-salinity inclusions are interpreted as primary and parallel to the growth zones, whereas the group with the higher salinity corresponds to inclusions in secondary trails. Some inclusions were not clearly linked to either growth zones or trails and thus could not be classified as primary or secondary. Their homogenization temperature data are included in Fig. 6.

283 °C for the low-salinity primary inclusions. No good correlation exists between salinity and homogenization temperatures for these inclusions. Fig. 7 displays the two groups of inclusions, separated according to their salinity: Inclusions with lower salinity and parallel to growth lines are primary, whereas those with high salinity located in trails are secondary.

3.5. Microthermometry on the Cabeça de Negro deposit

CO_2 melting temperatures are lower than −56.6 °C, mostly distributed around −57 and −59 °C (Fig. 5). These temperatures indicate that the carbonic phase is not pure. CO_2-phase homogenization into liquid state ranged from 17 to 29 °C. Clathrate dissolution was easily observed between 2.0° and 9.5 °C, implying a salinity range from 2 to 6 wt% NaCl equiv. Due to decrepitation, usually between 310 and 330 °C, only four total homogenization temperatures were obtained from the aqueous-carbonic fluid inclusions: three around 242 °C and one at 289 °C.

Similar to the Riacho Fundo deposit, aqueous inclusions can be separated into two groups in relation to their final ice-melting temperatures: one from −3.0 to −6.6 °C and another from −12.6 to −14.8 °C (Table 1), which are also equivalent to two salinity groups: low-salinity primary inclusions and high-salinity secondary inclusions (Fig. 7). In the Riacho Fundo deposit, the total homogenization temperatures of primary inclusions are variable, whereas the values for secondary inclusions tend to concentrate near higher values (>300 °C). In the Cabeça de Negro deposit, homogenization temperatures are the same for both types of inclusions, with lower values than those observed in the Riacho Fundo samples. Mean salinity is 8.0 wt% NaCl equiv. for primary inclusions and 18 wt% NaCl equiv. for secondary inclusions.

4. Discussion and conclusions

The study of fluid inclusions in magnesite is uncommon because usually inclusions are too small or of secondary nature. For example, Bone (1983) suggests that temperature is the major control of two distinctive magnesite morphologies at Rum Jungle, Australia. Rhombohedral magnesite recrystallized in association with aqueous, saturated fluid inclusions that display homogenization temperatures, mostly lower than 150 °C. Tabular magnesite, in contrast, formed by recrystallization at higher temperatures, probably during late-stage diagenesis of what was likely a primary magnesite. Fernandez-Nieto et al. (2003) study magnesite in a non-metamorphic, Late Ordovician dolomite formation in Spain and exclusively describe aqueous, two-phase fluid inclusions with no CO_2. Homogenization temperatures for these inclusions vary from 100 to 150 °C, with salinities ranging from 18.8 to 22.2 wt% NaCl equiv. in the Mg–Fe carbonates. Metasomatic hydrothermal replacement of a dolomite protolith resulted from the interaction between hot (100–150 °C) and saline (20 wt% NaCl equiv.), iron-rich hydrothermal fluids and marine carbonates. Velasco et al. (1987) study Paleozoic magnesite deposits at Eugui, Spain, and find two-phase fluid inclusions with liquid hydrocarbon and high contents of CH_4 in a low- to very low-grade metamorphic setting. Homogenization temperatures ranged between 140 and 300 °C, and the freezing point depression was not observed. The genetic model proposed by these authors involved an early Mg concentration (syndiagenetic dolomitization) during sedimentation and the formation of magnesite under diagenetic conditions, at low pressure and temperatures around 150 °C. Fluid inclusion data were compatible with low- to very low-grade metamorphic conditions. Lugli et al. (2002) describe the contribution from sedimentary, hydrothermal, and metasomatic sources to magnesite from the Upper Triassic Burano evaporites. Aqueous and saturated fluid inclusions were observed only in hydrothermal, vein-filling sparry magnesite, with total homogenization temperatures between 120 and 318 °C and salinity

around 30 wt% NaCl equiv. No CO_2 was described. The presence of micro-inclusions of Ca-bearing minerals was considered a result of replacement of a dolomite precursor. Metamorphic reactions were probably the fluid source.

Magnesite-rich marbles result from several periods of deformation and reequilibration and may contain a wide range of fluids with different compositions and origins formed at different times (Guedes et al., 2002). The characteristics of related fluids change over the duration of the metamorphic event, which involves recrystallization, renewed dissolution, and/or precipitation of new mineral assemblages (Winter, 2001). As observed in magnesite from Orós, primary, pseudo-secondary, and secondary fluid inclusions represent the only direct, though incomplete, evidence of these many phases (Roedder, 1984). A pure limestone ($CaCO_3$), when submitted to metamorphism, gradually undergoes recrystallization, forming larger calcite crystals in response to rising temperatures and finally becoming a marble (Miyashiro, 1973). However, magnesite in siliceous carbonate sediments is completely consumed during metamorphism. Only if magnesite is present in excess can it be preserved during higher-grade regional metamorphism (Winkler, 1979). The distribution, composition, and physical–chemical characteristics of the aqueous and aqueous-carbonic inclusions in the studied samples from the Riacho Fundo and Cabeça de Negro (Fig. 7) deposits are compatible with the evolution of the metamorphic processes on magnesite.

Clear, fluid inclusion-free crystals, such as those in Figs. 2 and 4, usually indicate slow, steady growth conditions during different processes, such as metamorphic recrystallization. The presence of remnant, solid dolomite micro-inclusions, whether associated with CO_2, hydrocarbon, or bitumen or not, results from either replacement or a change in fluid composition, likely heterogeneous. The preservation of sedimentary structures such as stromatolites and bitumen is not uncommon (Dutkiewicz et al., 2003; Munz et al., 1995), though any high-hydrocarbon organic matter originally present likely decomposes a few single volatiles such as CH_4 during metamorphism. Overall, the three major volatiles present in low- to medium-grade metamorphic rocks are H_2O, CO_2, and CH_4, in decreasing order of abundance, but N_2 or H_2S may also be abundant (Roedder, 1984; Winter, 2001).

According to Spear (1993), progressive metamorphism of the SiO_2–CaO–MgO system can generate H_2O and CO_2. These fluids, in equilibrium with carbonate rocks during metamorphism, can be nearly pure or constitute a mixture of both components in any proportion. In addition, H_2O and CO_2-bearing fluids can coexist in different parts of the same terrain during the same metamorphic event (Ferry and Burt, 1986). These interpretations reflect observations of fluid inclusions in magnesite from the Orós belt.

Data on the distribution of total homogenization temperatures obtained from aqueous inclusions (Figs. 6 and 7) show that temperatures in the Riacho Fundo are higher than in the Cabeça de Negro ore deposit. This difference is probably due to the different metamorphic degrees attained locally for each ore deposit. The vertical correlation observed in primary fluid inclusions from Riacho Fundo suggests either temperature changes or a pressure drop. Considering the geological setting of these samples, it seems reasonable to relate the data to metamorphic heating and subsequent fluid devolatilization, reequilibration, dissolution, and/or precipitation related to the metamorphic process. Likewise, the increasing homogenization temperatures and salinity observed from the aqueous primary to the secondary inclusions (Fig. 7), and subsequently the CO_2 appearance, are consistent with a change from low to high metamorphic grade (Roedder, 1984).

If the pressure estimated by Parente (1995) is taken into account, using information from Roedder (1984, p. 262), homogenization temperatures of the aqueous inclusions should be corrected by adding at least 170 °C, yielding data compatible with greenschist to amphibolite facies, as well as consistent with data from Sá (1991).

Sometimes aqueous-carbonic inclusions with lower CO_2 melting temperatures (e.g. −60 and −59 °C) are locally associated with solid accidental dolomite inclusions and organic material (bitumen?). According to Tucker (1991), there is a color change toward black during methane (CH_4) generation with increasing temperature and organic metamorphic grade. In this case, it seems reasonable to suppose that the aqueous-carbonic fluid inclusions could have been contaminated by methane during metamorphism, which would explain the irregular distribution of pure and volatile-rich CO_2 inclusions verified during microthermometric runs.

The presence of organic matter-bearing inclusions, probably hydrocarbon metamorphosed to bitumen, reinforces the syngenetic sedimentary genetic model in a marine evaporitic context, as proposed by Parente et al. (1998a,b, 2004). Dutkiewicz et al. (2003) note that in a suitable geological environment, relicts of aromatic compounds and bitumen, formed at low temperatures early in the burial history, can survive temperatures of up to 350 °C. Homogenization temperatures between 170 and 370 °C relate to the metamorphic process that recrystallized the primary sedimentary magnesite.

Nevertheless, the identification of volatiles such as CH_4 by Raman spectrometry in aqueous carbonic inclusions remains problematic. This limitation is probably due to the small number of analyzed fluid inclusions.

Acknowledgments

We are grateful to Barbara Fonseca, Paulo José Martins Filho, and Janice Caldas Araujo for helping with the microthermometric runs. We appreciate the suggestions from the two reviewers, Gaston Giuliani and Roberto P. Xavier, which helped substantially improve the manuscript.

References

Bodnar, R.J., 2003. Introduction to aqueous-electrolyte fluid inclusions. In: Samson, I., Anderson, A., Marshall, D. (Eds.), Fluid Inclusions – Analysis and interpretation, vol. 32. Mineralogical Association of Canada Short Course Series, Vancouver, pp. 81–100.

Bone, Y., 1983. Interpretation of magnesites at Rum Jungle, N T., using fluid inclusions. Journal of the Geological Society of Australia 30, 375–381.

Brown, P.E., Hagemann, S.G., 1994. MacFlinCor: a computer program for fluid inclusion data reduction and manipulation. In: De Vivo, B., Frezzotti, M.L. (Eds.), Fluid Inclusions in Minerals: Methods and Applications. Virginia Tech, Blaksburg, pp. 231–250.

Brown, P.E., Lamb, W.M., 1986. Mixing of H_2O–CO_2 in fluid inclusions: geobarometry and Archean gold deposits. Geochimica et Cosmochimica Acta 50, 847–852.

Chaye d'Albissin, M., Guillou, J.J., 1985. La conservation de microorganismes dans une manésitite spathique et ses incidences cristallogénétiques et sédimentologiques. Comptes Rendus Academie Sciences Paris, t.301, série II 11, 797–799.

Dabitzias, S.G., 1980. Petrology and genesis of the Vavdos cryptocrystalline magnesite deposits, Chalkidi peninsula, northern Greece. Economic Geology 75, 1138–1151.

Dutkiewicz, A., Ridley, J., Buick, R., 2003. Oil-bearing CO_2–CH_4–H_2O fluid inclusions: oil survival since the Paleoproterozoic after high temperature entrapment. Chemical Geology 194, 51–79.

Fernandez-Nieto, C., Torrez Ruiz, J., Subias Pérez, I., Fanlo González, I., González López, J.M., 2003. Genesis of Mg–Fe Carbonates from the Sierra Menera magnesite–siderite deposits, northeast Spain: evidence from fluid inclusions, trace elements, rare earth elements, and stable isotope data. Economic Geology 98, 1413–1426.

Feraud, G.L.F., Caby, R., Vauchez, A., Corsini, M., Arthaud, M., Archanjo, C.J., Jardim de Sá, E.F., Egidio da Silva, M., 1992. O sincronismo termo- tectônico polifásico Brasiliano dos sistemas cisalhantes Patos-Seridó e Campina Grande (Província Borborema) à luz de datações 40Ar/39Ar de mono-cristais com sonda-laserCongresso Brasileiro de Geologia, 37. Anais, São Paulo, Sociedade Brasileira de Geologia, pp. 378–379.

Ferry, J.M., Burt, D.M., 1986. Characterization of metamorphic fluid composition through mineral equilibria. In: Ferry, J.M. (Ed.), Characterization of metamorphism through mineral equilibria Reviews in Mineralogy, 10. Mineralogical Society of America, pp. 207–262.

Guedes, A., Noronha, F., Boiron, M-C., Banks, D.A., 2002. Evolution of fluids associated with metasedimentary sequences from Chaves (north Portugal). Chemical Geology 190, 273–289.

Kerkhof, A.M. van den, 1988. The system CO_2–CH_4–N_2 in fluid inclusions: theoretical modelling and geological applications. Free University Press, Amsterdam, 206 pp.

Lugli, S., Morteani, G., Blamart, D., 2002. Petrographic, REE, fluid inclusion and stable isotope study of magnesite from the upper Triassic Burano evaporites (Secchia Valley, northern Apennines): contributions from sedimentary, hydrothermal and metasomatic sources. Mineralium Deposita 37, 480–494.

McMillan, P.F., 1989. Raman spectroscopy in mineralogy and geochemistry. Annual Review of Earth and Planetary Sciences 17, 255–283.

Miyashiro, A., 1973. Metamorphism and metamorphic belts. George Allen and Unwin, London, 492 pp.

Morteani, G., 1989. Fluid inclusions in magnesiteMonograph Series on Mineral Deposits, 28. Gebruder Borntraeger, Berlin, Stuttgart, pp. 237–239.

Munz, I.A., Yardley, B.W.D., Banks, D.A., Wayne, D., 1995. Deep penetration of sedimentary fluids in basement rocks from southern Norway: evidence from hydrocarbon and brine inclusions in quartz veins. Geochimica et Cosmochimica Acta 59, 239–254.

Parente, C.V., 1995. Géologie e paléogéographie d'une plate-forme à évaporites et magnesite d'âge proterozoïque: le cadre géotectonique initial de la ceinture mobile Orós dans la region d'Alencar (Ceará – Brésil). Thèse de doctorat de l'Université de Nantes, 306 pp.

Parente, C.V., Arthaud, M.H., 1995. O sistema Orós – Jaguaribe no Ceará, NE do Brasil. Revista Brasileira de Geociências 25, 297–305.

Parente, C.V., Guillou, J.J., Carvalho Júnior, L.E., 1998a. Comportamento geoquímico dos elementos terras raras da seqüência metacarbonática magnesiana pré-cambriana (~1,8 Ga) da Faixa Móvel Orós. Revista Brasileira de Geociências 28, 431–438.

Parente, C.V., Guillou, J.J., Arthaud, M.H., 1998b. Geologia e geoquímica dos elementos maiores dos depósitos de magnesita pré-cambriana (~1,8 Ga) da Faixa Móvel Orós (Ceará). Revista Brasileira de Geociências 28, 439–448.

Parente, C.V., Ronchi, L.H., Sial, A.N., Guillou, J.G., Arthaud, M.H., Fuzikawa, K., Veríssimo, C.U.V., 2004. Geology and geochemistry of Paleoproterozoic magnesite deposits (~1.8 Ga), state of Ceará, Northeastern Brazil. Carbonates and Evaporites 19, 28–50.

Pironon, J., 1991. Apport des techniques microspectroscopiques a Íétude des inclusions hydrocarbonées intracristallines. Thèse de ÍUniversité de Nancy I, France, 235pp.

Pironon, J., Rochdi, A., Barres, O., Burneau, A., Landais, P., Pagel, M., Poty, B., 1991. Applications of FT-IR microspectroscopy in the earth sciences. In: Proceedings of the International Workshop on Fourier Transform Spectroscopy. Antwerp, Belgium, pp. 281–291.

Roedder, E., 1984. Fluid inclusions. In: Ribbe, P.H. (Ed.), Reviews in Mineralogy. Mineralogical Society of America, p. 644 pp.

Ronchi, L.H., Bény, C., 1997. Espectroscopia Raman: Aplicações em Geologia e Limitações. Acta Geologica Leopoldensia 44, 5–25.

Sá, J.M., 1991. Évolution géodynamique de la ceinture proterozoique dOrós, Nord-est du Brésil. Thèse de Doctorat de ÍUniversité de Nancy. I, 117 pp.

Spear, F.S., 1993. Metamorphic phase equilibria and pressure-temperature-time paths. Mineralogical Society of America Monograph, Washington, 799 pp.

Tucker, M.E., 1991. Sedimentary petrology, an introduction to the origin of sedimentary rocks. Blackwell Scientific Publications, Oxford, 260 pp.

Van Schmus, W.R., Brito Neves, B.B., Hackspacher, P., Babinski, M., 1995. U/Pb and Sm/Nd geochronologic studies of the easthern Borborema Province, Northeastern Brazil: initial conclusions. Journal of South American Earth Sciences 8, 267–288.

Velasco, F., Pesquera, A., Arce, R., Olemdo, F., 1987. A contribution to the ore genesis of the magnesite deposit of Eugui, Navarra (Spain). Mineralium Deposita 22, 33–41.

Winkler, H.G.F., 1979. Petrogenesis of metamorphic rocks. Springer, Berlin Heidelbreg New York, 348 pp.

Winter, J.D., 2001. An introduction to igneous and metamorphic petrology. Prentice Hall, Upper Saddle River, New Jersey, 697 pp.